

# Effective Reinforcement Learning Control using Conservative Soft Actor-Critic

Xinyi Yuan<sup>1,3,†</sup>, Zhiwei Shang<sup>1,3,†</sup>, Wenjun Huang<sup>2</sup>, Yunduan Cui<sup>2</sup>, Di Chen<sup>1,3</sup>,  
Meixin Zhu<sup>1,3,4,\*</sup>

**Abstract**—Reinforcement Learning (RL) has shown great potential in complex control tasks, particularly when combined with deep neural networks within the Actor-Critic (AC) framework. However, in practical applications, balancing exploration, learning stability, and sample efficiency remains a significant challenge. Traditional methods such as Soft Actor-Critic (SAC) and Proximal Policy Optimization (PPO) address these issues by incorporating entropy or relative entropy regularization, but often face problems of instability and low sample efficiency. In this paper, we propose the Conservative Soft Actor-Critic (CSAC) algorithm, which seamlessly integrates entropy and relative entropy regularization within the AC framework. CSAC improves exploration through entropy regularization while avoiding overly aggressive policy updates with the use of relative entropy regularization. Evaluations on benchmark tasks and real-world robotic simulations demonstrate that CSAC offers significant improvements in stability and efficiency over existing methods. These findings suggest that CSAC provides strong robustness and application potential in control tasks under dynamic environments.

**Note to Practitioners**— This paper addresses the challenges of applying Reinforcement Learning (RL) in real-world automation tasks, particularly in maintaining stability and efficiency during the training process. Traditional RL methods like SAC and PPO often suffer from instability or require a large number of samples. The proposed Conservative Soft Actor-Critic (CSAC) algorithm balances exploration and exploitation by integrating entropy and relative entropy regularization. Practitioners working in fields such as robotic arms, unmanned systems, or manufacturing can apply CSAC to improve training efficiency and stability in dynamic environments. While CSAC has shown excellent performance in simulations, further research is needed to assess its effectiveness in large-scale real-world environments, particularly in systems with real-time constraints.

## I. INTRODUCTION

**R**EINFORCEMENT Learning (RL) has emerged as a powerful method for learning optimal control strategies in complex and dynamic environments, distinguished by its unique ability to operate without relying on prior knowledge [1]. By continuously interacting with the environment, RL algorithms autonomously develop strategies that excel across a broad spectrum of tasks, ranging from robotic control to game playing [2]–[7]. Particularly, when deep neural networks [8] are combined with the Actor-Critic (AC)

architecture [9], RL’s capability to handle high-dimensional state and action spaces is significantly enhanced, enabling it to achieve superhuman performance in numerous challenging domains [10]–[15].

However, applying RL to real-world systems presents several critical challenges, particularly in balancing sample efficiency, learning stability, and overall control performance [16]–[18]. If these aspects are not adequately managed, the training process may incur prohibitive costs and result in unreliable control behaviors. To address these challenges, researchers have explored various regularization techniques, such as entropy or relative entropy, which have shown significant effectiveness in optimizing the trade-off between exploration and exploitation in RL algorithms.

Soft Actor-Critic (SAC) [19], as one of the classical methods in Maximum Entropy Reinforcement Learning (MERL), introduces an entropy regularization term in the objective function to promote broad exploration of the policy space. This approach has demonstrated exceptional performance across various control tasks [20]–[23], primarily due to its incentive for exploration during policy optimization. However, in the pursuit of maximizing policy entropy, SAC’s learning process can sometimes be destabilized, particularly in scenarios where the dynamics of the policy and entropy are misaligned or where the environment undergoes significant changes. Such instability can lead to overly aggressive policy updates, adversely affecting the efficiency and effectiveness of policy convergence.

In contrast, methods such as Trust Region Policy Optimization (TRPO) [24] and Proximal Policy Optimization (PPO) [25] employ relative entropy as a constraint to limit the magnitude of policy updates, thereby effectively reducing instability during the learning process. This approach prevents the dramatic fluctuations that can occur due to overly large policy updates, ensuring greater learning stability. However, this stability often comes at the cost of sample efficiency, particularly in on-policy settings, where the algorithm requires a larger number of samples to achieve effective learning [26]–[29]. This increased sample demand becomes especially pronounced in complex scenarios that are difficult to simulate or parallelized.

Although the aforementioned methods offer valuable insights into balancing stability and exploration, and entropy or relative entropy based RL methods have shown great potential in practical applications, there remains a relative paucity of research on effectively integrating entropy and relative entropy regularization within an AC framework, particularly in the context of continuous control tasks. Previous research, such as Dynamic Policy Programming (DPP) [31] and Conservative

<sup>†</sup>Zhiwei Shang and Xinyi Yuan have contributed equally to this work.

\* Corresponding author: Meixin Zhu (e-mail: meixin@ust.hk)

<sup>1</sup> Intelligent Transportation Thrust, Systems Hub, The Hong Kong University of Science and Technology (Guangzhou), Guangzhou, China

<sup>2</sup> Shenzhen Institute of Advanced Technology, Chinese Academy of Sciences, Shenzhen, China.

<sup>3</sup> Guangdong Provincial Key Lab of Integrated Communication, Sensing and Computation for Ubiquitous Internet of Things, Guangzhou, China.

<sup>4</sup> Department of Civil and Environmental Engineering, The Hong Kong University of Science and Technology, Hong Kong SAR, China.

TABLE I  
COMPARISON OF CSAC AND THE RELATED APPROACHES

Approach	Entropy	Relative Entropy
TD3 [30]	×	×
PPO [25]	×	○
SAC [19]	○	×
CSAC (ours)	○	○

Value Iteration (CVI) [32], has demonstrated the significant advantages of incorporating these regularization techniques in value-based RL methods. Moreover, extensions of these algorithms further underscore the strong potential of these techniques for engineering applications [33]–[36]. However, the computational complexity associated with SoftMax operations in continuous action spaces has largely confined these methods to discrete action spaces, limiting their applicability to broader real-world scenarios.

To overcome the limitations of existing methods, this paper proposes a novel reinforcement learning algorithm, Conservative Soft Actor-Critic (CSAC), which seamlessly integrates entropy and relative entropy regularization within an AC framework. CSAC employs a conservative policy update mechanism that effectively balances exploration and exploitation, significantly enhancing learning stability and sample efficiency. Specifically, CSAC is designed with a specialized Q-function in the critic, utilizing entropy regularization to enhance exploration capabilities, while relative entropy regularization is used to prevent overly aggressive policy updates, thereby ensuring robustness in complex environments. According to the relationship of related works concluded in Table I, the contributions of this paper are summarized as:

- 1) We develop an innovative RL method that organically combines entropy and relative entropy regularization, incorporating the stability of PPO and the high exploration capability of SAC. This method demonstrates significant improvements in sample efficiency and learning stability across various control tasks, validating its effectiveness in different task environments.
- 2) We successfully extend the principles of Conservative Value Iteration (CVI) and Dynamic Policy Programming (DPP) to continuous action spaces and implement this extension within the AC structure without introducing additional computational complexity. This advancement greatly expands the applicability of entropy-constrained RL methods in practical scenarios, providing new solutions for complex continuous control tasks.
- 3) Through extensive experiments on various benchmark control tasks and Real-Robot-Based simulations, we systematically validate the effectiveness of CSAC. The experimental results show that CSAC significantly outperforms existing mainstream RL algorithms in terms of learning stability, sample efficiency, and final policy performance, demonstrating its potential and advantages in complex control tasks.

## II. PRELIMINARIES

### A. Markov Decision Processes

The interaction between the environment and RL agent is usually formulated as a Markov Decision Process (MDP) with a 5-tuple  $(\mathcal{S}, \mathcal{A}, r, \mathcal{P}, \gamma)$ .  $\mathcal{S}$  and  $\mathcal{A}$  denote the spaces of state  $s$  and action  $a$ . The reward function designed for a specific task is  $r(s, a)$ . The transition probability from one state to another one under a given action is defined as  $\mathcal{P} : \mathcal{S} \times \mathcal{S} \times \mathcal{A} \mapsto [0, 1]$ .  $\gamma \in [0, 1)$  is the discount factor to gradually ignore the reward in a long horizon. The policy  $\pi : \mathcal{S} \times \mathcal{A} \mapsto [0, 1]$  maps state space to a probability distribution over the action space. Define  $s_0 = s$ ,  $a_t \sim \pi(\cdot|s_t)$ ,  $a_0 = a$ ,  $s_{t+1} \sim \mathcal{P}(\cdot|s_t, a_t)$ , the objective of the traditional RL method is to obtain an optimal policy that maximizes the reward obtained in a long term. It is defined as the value function  $V(\cdot)$ :

$$V_\pi(s) = \mathbb{E}_\pi \left[ \sum_{t=0}^{\infty} \gamma^t r(s_t, a_t) \right]. \quad (1)$$

It can be translated to the following Bellman equation:

$$V_\pi(s) = \sum_{a \in \mathcal{A}} \pi(a|s) \left[ r(s, a) + \gamma \sum_{s' \in \mathcal{S}} \mathcal{P}(s'|s, a) V_\pi(s') \right]. \quad (2)$$

Let  $s' \sim \mathcal{P}(s'|s, a)$ ,  $a' \sim \pi(a'|s')$ , the equation above can be translated regarding to the state-action pair:

$$Q_\pi(s, a) = r(s, a) + \gamma \mathbb{E}_{s', a'} [Q_\pi(s', a')]. \quad (3)$$

### B. Actor-Critic Framework

The Actor-Critic (AC) framework is a key structure in RL, effectively integrating policy-based and value-based approaches. The framework consists of two components: the Actor, which represents the policy  $\pi(a|s; \phi)$ , and the Critic, which estimates the value function  $V(s; \theta)$  or the action-value function  $Q(s, a; \theta)$ . The Actor updates the policy by following the gradient of expected return, while the Critic improves the value function estimate to provide better feedback to the Actor.

During each interaction with the environment, the Actor selects an action  $a_t$  based on the current policy  $\pi(a_t|s_t; \phi)$ , resulting in a transition to the next state  $s_{t+1}$  and receiving a reward  $r_t$ . The Critic evaluates the action by computing the Temporal Difference (TD) error:

$$\delta_t = r_t + \gamma V(s_{t+1}; \theta) - V(s_t; \theta) \quad (4)$$

The Actor updates its policy parameters  $\phi$  using the gradient of the expected return:

$$\phi \leftarrow \phi + \alpha \nabla_\phi \log \pi(a_t|s_t; \phi) \delta_t \quad (5)$$

The Critic updates its parameters  $\theta$  to minimize the TD error:

$$\theta \leftarrow \theta - \beta \nabla_\theta [\delta_t^2] \quad (6)$$

The AC framework serves as the foundation for several advanced RL algorithms such as DDPG [37], SAC and PPO, demonstrating its versatility and effectiveness in various control tasks.

### III. APPROACH

#### A. Mix Entropy and Relative Entropy in Value Function

In this section, we introduce the proposed Conservative Soft Actor-Critic (CSAC) method, which builds upon the foundation of the value function by incorporating both entropy and relative entropy regularization. The reward function within the CSAC framework is defined as follows:

$$r_{\text{CSAC}}(\mathbf{s}_t, \mathbf{a}_t) = r(\mathbf{s}_t, \mathbf{a}_t) + \gamma \sigma \mathbb{E}_{\mathbf{s}_{t+1}} [-\log(\pi(\cdot|\mathbf{s}_{t+1}))] - \gamma \tau \mathbb{E}_{\mathbf{s}_{t+1}} \left[ \log \frac{\pi(\cdot|\mathbf{s}_{t+1})}{\tilde{\pi}(\cdot|\mathbf{s}_{t+1})} \right]. \quad (7)$$

In this expression, the second term represents entropy regularization, modulated by the parameter  $\sigma$ , while the third term accounts for relative entropy regularization, controlled by the parameter  $\tau$ . By introducing the reward function defined in Eq. (7) into the value function equation (Eq. (3)), we derive the corresponding value function for CSAC as follows:

$$Q_{\text{CSAC}}(\mathbf{s}_t, \mathbf{a}_t) = r(\mathbf{s}_t, \mathbf{a}_t) + \gamma \mathbb{E}_{\mathbf{s}_{t+1}, \mathbf{a}_{t+1}} [Q_{\text{CSAC}}(\mathbf{s}_{t+1}, \mathbf{a}_{t+1}) - \sigma \log(\pi(\mathbf{a}_{t+1}|\mathbf{s}_{t+1})) - \tau \log \frac{\pi(\mathbf{a}_{t+1}|\mathbf{s}_{t+1})}{\tilde{\pi}(\mathbf{a}_{t+1}|\mathbf{s}_{t+1})}] \quad (8)$$

To address potential overestimation issues commonly observed in value-based methods, similar to approaches employed in Delayed Deep Deterministic Policy Gradient (TD3) [30] and Soft Actor-Critic (SAC) [19], we utilize two critic networks,  $Q_{\text{CSAC}}^{\theta_1}$  and  $Q_{\text{CSAC}}^{\theta_2}$ , each with independent weights, to approximate  $Q_{\text{CSAC}}(\cdot)$ .

Given a sample from the dataset  $\{\mathbf{s}, \mathbf{a}, r(\mathbf{s}, \mathbf{a}), \mathbf{s}'\} \sim \mathcal{D}$ , the TD error is defined as  $y(\mathbf{s}, \mathbf{a}, \mathbf{s}')$ , where  $\mathbf{a}' \sim \pi(\cdot|\mathbf{s}')$ . The loss function for the critic in CSAC is then formulated as:

$$L(\theta_i) = \left[ Q_{\text{CSAC}}^{\theta_i}(\mathbf{s}, \mathbf{a}) - y(\mathbf{s}, \mathbf{a}, \mathbf{s}') \right]^2, \quad i \in \{1, 2\} \quad (9)$$

where the TD target  $y(\mathbf{s}, \mathbf{a}, \mathbf{s}')$  is computed as:

$$y(\mathbf{s}, \mathbf{a}, \mathbf{s}') = r(\mathbf{s}, \mathbf{a}) + \gamma \left[ \min_{j=1,2} Q_{\text{CSAC}}^{\theta_j}(\mathbf{s}', \mathbf{a}') - \sigma \log(\pi(\mathbf{a}'|\mathbf{s}')) - \tau \log \frac{\pi(\mathbf{a}'|\mathbf{s}')}{\tilde{\pi}(\mathbf{a}'|\mathbf{s}')} \right] \quad (10)$$

In this formulation, the TD error is derived by taking the minimum value across the two target critic networks, denoted by parameters  $\theta$ . The action  $\mathbf{a}'$  is sampled from the current policy  $\pi(\cdot|\mathbf{s}')$ , while the previous policy  $\tilde{\pi}(\cdot|\mathbf{s}')$  is iteratively stored and updated during the learning process. This design choice helps to stabilize the learning process and mitigate the risk of overfitting to the current policy.

#### B. Policy Improvement with Mixed Entropy and Relative Entropy Regularization

Next, we derive the updated formulation of the corresponding actor networks. To begin, we first express the optimal version of Eq. (8) as follows:

$$Q_{\text{CSAC}}^*(\mathbf{s}_t, \mathbf{a}_t) = r(\mathbf{s}_t, \mathbf{a}_t) + \gamma \max_{\pi} \mathbb{E}_{\mathbf{s}_{t+1}} [Q_{\text{CSAC}}^*(\mathbf{s}_{t+1}, \mathbf{a}_{t+1}) - \sigma \log(\pi(\mathbf{a}_{t+1}|\mathbf{s}_{t+1})) - \tau \log \frac{\pi(\mathbf{a}_{t+1}|\mathbf{s}_{t+1})}{\tilde{\pi}(\mathbf{a}_{t+1}|\mathbf{s}_{t+1})}]. \quad (11)$$

This expression can be further simplified by leveraging the equivalence between the value and action-value functions:

$$Q(\mathbf{s}_t, \mathbf{a}_t) = r(\mathbf{s}_t, \mathbf{a}_t) + \gamma \mathbb{E}_{\mathbf{s}_{t+1}} [V(\mathbf{s}_{t+1})]. \quad (12)$$

Following the approach in SAC [19], the optimal value function is then given by:

$$V_{\text{CSAC}}^*(\mathbf{s}_t) = \max_{\pi} \sum_{\mathbf{a}_t \in \mathcal{A}} \pi(\mathbf{a}_t|\mathbf{s}_t) \left[ Q_{\text{CSAC}}^*(\mathbf{s}_t, \mathbf{a}_t) - \sigma \log(\pi(\mathbf{a}_t|\mathbf{s}_t)) - \tau \log \frac{\pi(\mathbf{a}_t|\mathbf{s}_t)}{\tilde{\pi}(\mathbf{a}_t|\mathbf{s}_t)} \right]. \quad (13)$$

Consequently, the optimal policy for any given state  $\mathbf{s}$  becomes:

$$\pi^* = \arg \max_{\pi} \sum_{\mathbf{a} \in \mathcal{A}} \pi(\mathbf{a}|\mathbf{s}) \left[ Q_{\text{CSAC}}^*(\mathbf{s}, \mathbf{a}) - \sigma \log(\pi(\mathbf{a}|\mathbf{s})) - \tau \log \frac{\pi(\mathbf{a}|\mathbf{s})}{\tilde{\pi}(\mathbf{a}|\mathbf{s})} \right]. \quad (14)$$

For continuous action spaces, based on the constraints  $0 < \pi(\mathbf{a}|\mathbf{s}) < 1$  and  $\int \pi(\mathbf{a}|\mathbf{s}) d\mathbf{a} = 1$ , together with Eq. (14), we construct a Lagrangian function as follows:

$$\mathcal{L}(\mathbf{s}, \lambda) = \int \pi(\mathbf{a}|\mathbf{s}) \left[ Q_{\text{CSAC}}(\mathbf{s}, \mathbf{a}) + \sigma [-\log(\pi(\mathbf{a}|\mathbf{s}))] - \tau \left[ \log \frac{\pi(\mathbf{a}|\mathbf{s})}{\tilde{\pi}(\mathbf{a}|\mathbf{s})} \right] \right] d\mathbf{a} - \lambda \left( \int \pi(\mathbf{a}|\mathbf{s}) d\mathbf{a} - 1 \right). \quad (15)$$

The partial derivative of this Lagrangian function with respect to  $\pi(\mathbf{a}|\mathbf{s})$  is given by:

$$Q_{\text{CSAC}}(\mathbf{s}, \mathbf{a}) - \sigma - \sigma \log \pi(\mathbf{a}|\mathbf{s}) - \tau - \tau \log \frac{\pi(\mathbf{a}|\mathbf{s})}{\tilde{\pi}(\mathbf{a}|\mathbf{s})} - \lambda = 0. \quad (16)$$

Following the method in CVI [32], we define  $\alpha = \frac{\tau}{\tau + \sigma}$  and  $\beta = \frac{1}{\tau + \sigma}$ , and express the policy as:

$$\pi(\mathbf{a}|\mathbf{s}) = \tilde{\pi}^\alpha(\mathbf{a}|\mathbf{s}) e^{(-\beta\lambda - 1)} e^{\beta Q_{\text{CSAC}}(\mathbf{s}, \mathbf{a})}. \quad (17)$$

The parameter  $\lambda$  can be computed using the normalization condition  $\int \pi(\mathbf{a}|\mathbf{s}) d\mathbf{a} = 1$ , which yields:

$$\int \pi(\mathbf{a}|\mathbf{s}) d\mathbf{a} = \int \tilde{\pi}^\alpha(\mathbf{a}|\mathbf{s}) e^{-\beta\lambda - 1} e^{\beta Q_{\text{CSAC}}(\mathbf{s}, \mathbf{a})} d\mathbf{a} = 1, \\ \lambda = \frac{\log \left[ \int \tilde{\pi}^\alpha(\mathbf{a}|\mathbf{s}) \exp(\beta Q_{\text{CSAC}}(\mathbf{s}, \mathbf{a})) d\mathbf{a} \right]}{\beta} - \frac{1}{\beta}. \quad (18)$$

By combining Eqs. (18) and (17), we obtain the updated policy:

$$\pi_{k+1}(\mathbf{a}|\mathbf{s}) = \frac{\pi_k^\alpha(\mathbf{a}|\mathbf{s}) \exp(\beta Q_{\text{CSAC},k+1}(\mathbf{s}, \mathbf{a}))}{\int \pi_k^\alpha(\mathbf{a}|\mathbf{s}) \exp(\beta Q_{\text{CSAC},k+1}(\mathbf{s}, \mathbf{a})) d\mathbf{a}}, \quad (19)$$

where  $k$  indicates the iteration number, and  $\pi_{k+1}$  and  $\pi_k$  denote the current and previous policies, respectively. This expression can be further simplified by introducing the action preference function  $P$  [1], [31]:

$$P_{k+1}(\mathbf{s}, \mathbf{a}) = \frac{\alpha}{\beta} \log \pi_k(\mathbf{a}|\mathbf{s}) + Q_{\text{CSAC},k+1}(\mathbf{s}, \mathbf{a}), \quad (20)$$

$$V_{\text{CSAC},k}(\mathbf{s}) = \frac{1}{\beta} \log \int \exp(\beta P_k(\mathbf{s}, \mathbf{a})) d\mathbf{a}, \quad (21)$$

$$\pi_k(\mathbf{a}|\mathbf{s}) = \exp(\beta (P_k(\mathbf{s}, \mathbf{a}) - V_{\text{CSAC},k}(\mathbf{s}))). \quad (22)$$

According to SAC [19], Eq. (19) conforms to the Energy-Based Policy (EBP) model. However, this EBP cannot be sampled directly like a typical Gaussian distribution. Therefore, we substitute a Gaussian distribution for the EBP to interact with the environment, and aim to approximate this Gaussian distribution to the EBP during policy optimization [19], [38]. The distance between the agent's strategy and the EBP is measured using the KL divergence. Thus, given one state from the sample set  $\mathbf{s} \sim \mathcal{D}$ , the policy improvement in the actor networks controlled by parameters  $\phi$  is achieved by minimizing the following cost function:

$$J_\pi(\phi) = D_{\text{KL}}[\pi(\cdot | \mathbf{s}) \| \exp \beta (P(\mathbf{s}, \cdot) - V_{\text{CSAC}}(\mathbf{s}))] \\ = \mathbb{E}_{\mathbf{a} \sim \pi} [\log \pi(\mathbf{a}|\mathbf{s}) - \beta P(\mathbf{s}, \mathbf{a}) + \beta V_{\text{CSAC}}(\mathbf{s})]. \quad (23)$$

The output of actor networks in CSAC is defined, following SAC, to generate random control signals:

$$\tilde{\mathbf{a}}(\mathbf{s}, \boldsymbol{\xi}) = \tanh(\boldsymbol{\mu}(\mathbf{s}) + \boldsymbol{\sigma}(\mathbf{s}) \odot \boldsymbol{\xi}), \quad \boldsymbol{\xi} \sim \mathcal{N}(\mathbf{0}, \mathbf{I}), \quad (24)$$

where  $\boldsymbol{\mu}(\mathbf{s})$  and  $\boldsymbol{\sigma}(\mathbf{s})$  denote the mean and variance of the output signal. Dividing Eq. (23) by  $\beta$  and omitting the last term, which requires integration over the entire action space, the cost function for the actor networks can be approximated as:

$$J_\pi(\phi) \approx (\tau + \sigma) \log \pi(\tilde{\mathbf{a}}(\mathbf{s}, \boldsymbol{\xi})|\mathbf{s}) - \tau \log \tilde{\pi}(\tilde{\mathbf{a}}(\mathbf{s}, \boldsymbol{\xi})|\mathbf{s}) \\ - \min_{i=1,2} (Q_{\text{CSAC}}^{\theta_i}(\mathbf{s}, \tilde{\mathbf{a}}(\mathbf{s}, \boldsymbol{\xi}))), \quad (25)$$

where the action preference function is determined by the critic networks with the lower output:

$$P(\mathbf{s}, \tilde{\mathbf{a}}(\mathbf{s}, \boldsymbol{\xi})) = \tau \log \tilde{\pi}(\tilde{\mathbf{a}}(\mathbf{s}, \boldsymbol{\xi})|\mathbf{s}) + \min_{i=1,2} (Q_{\text{CSAC}}^{\theta_i}(\mathbf{s}, \tilde{\mathbf{a}}(\mathbf{s}, \boldsymbol{\xi}))). \quad (26)$$

---

**Algorithm 1: Conservative Soft Actor-Critic**


---

Initialize memory buffer  $\mathcal{D}$ , soft update rate  $\rho$ ,  $\sigma$  and  $\tau$  that control entropy and relative entropy terms, critic networks  $Q^{\theta_1}, Q^{\theta_2}$ , target critic networks  $Q^{\hat{\theta}_1}, Q^{\hat{\theta}_2}$  with copied parameters  $\hat{\theta}_1 \leftarrow \theta_1, \hat{\theta}_2 \leftarrow \theta_2$ , actor network  $\pi_\phi$  and previous actor networks  $\pi^{\phi_p}$  with current weights:  $\phi_p \leftarrow \phi$

**for**  $t = 1$  to  $T_{\text{initial}}$  **do**

  # Collect sample with a random policy  
   $\mathcal{D} \leftarrow (\mathbf{s}_t, \mathbf{a}_t, r(\mathbf{s}_t, \mathbf{a}_t), \mathbf{s}_{t+1})$

**for**  $t = 1$  to  $T$  **do**

  # Interaction phase

  Observe state  $\mathbf{s}_t$

  Decide and execute action  $\mathbf{a}_t \sim \pi^\phi(\mathbf{a}_t|\mathbf{s}_t)$

  Observe next state  $\mathbf{s}_{t+1}$  and get reward  $r(\mathbf{s}_t, \mathbf{a}_t)$

$\mathcal{D} \leftarrow (\mathbf{s}_t, \mathbf{a}_t, r(\mathbf{s}_t, \mathbf{a}_t), \mathbf{s}_{t+1})$

  # Update phase

$\phi_p \leftarrow \phi$

  Random sample mini-batch of  $M$  tuples from  $\mathcal{D}$

**for** each sampled tuple  $(\mathbf{s}, \mathbf{a}, r(\mathbf{s}, \mathbf{a}), \mathbf{s}')$  **do**

    # Calculate TD error following Eq. (10)

$\mathbf{a}' \sim \pi^\phi(\cdot|\mathbf{s}')$

$y(\mathbf{s}, \mathbf{a}, \mathbf{s}') = r(\mathbf{s}, \mathbf{a}) + \gamma(\min_{j=1,2} Q^{\theta_j}(\mathbf{s}', \mathbf{a}'))$

$-\sigma \log(\pi^\phi(\mathbf{a}'|\mathbf{s}')) - \tau \log \frac{\pi^\phi(\mathbf{a}'|\mathbf{s}')}{\pi_{\phi_p}(\mathbf{a}'|\mathbf{s}')})$

    # Update critic networks following Eq. (9)

$\nabla_{\theta_i} [Q^{\theta_i}(\mathbf{s}, \mathbf{a}) - y(\mathbf{s}, \mathbf{a}, \mathbf{s}')]^2$ , for  $i \in \{1, 2\}$

    # Update actor networks following Eq. (25)

$\nabla_{\phi} (\tau + \sigma) \log \pi^\phi(\tilde{\mathbf{a}}(\mathbf{s}, \boldsymbol{\xi})|\mathbf{s}) -$

$\tau \log \pi^{\phi_p}(\tilde{\mathbf{a}}(\mathbf{s}, \boldsymbol{\xi})|\mathbf{s}) - \min_{i=1,2} (Q^{\theta_i}(\mathbf{s}, \tilde{\mathbf{a}}(\mathbf{s}, \boldsymbol{\xi})))$

    # Update target networks weights

$\hat{\theta}_i \leftarrow \rho \theta_i + (1 - \rho) \hat{\theta}_i$  for  $i \in \{1, 2\}$

**return**  $Q^{\theta_1}(\cdot), Q^{\theta_2}(\cdot), \pi^\phi(\cdot)$

---

### C. Summary of Conservative Soft Actor-Critic

The entire learning process of the proposed Conservative Soft Actor-Critic (CSAC) algorithm is outlined in Algorithm 1. Initially, the critic networks  $Q^{\theta_1}, Q^{\theta_2}$  and the actor network  $\pi_\phi$  are initialized. The parameters of the critic networks are also duplicated to initialize the target networks  $Q^{\hat{\theta}_1}$  and  $Q^{\hat{\theta}_2}$ .

To begin the training, a random policy is employed for  $T_{\text{initial}}$  steps to collect a set of initial samples, which are stored in the replay buffer  $\mathcal{D}$ . During the learning process, at each timestep  $t$ , the CSAC algorithm first enters the interaction phase, where the current state  $\mathbf{s}_t$  is observed from the environment, and an action  $\mathbf{a}_t \sim \pi^\phi(\mathbf{a}_t|\mathbf{s}_t)$  is selected based on the actor network. Upon executing this action, the agent observes the next state  $\mathbf{s}_{t+1}$  and receives the corresponding reward  $r(\mathbf{s}_t, \mathbf{a}_t)$ . The experience tuple  $(\mathbf{s}_t, \mathbf{a}_t, r(\mathbf{s}_t, \mathbf{a}_t), \mathbf{s}_{t+1})$  is then added to the replay buffer  $\mathcal{D}$ .

In the subsequent update phase, the current parameters of the actor network are stored as the previous actor parameters. The agent then randomly samples a mini-batch of  $M$  experiences from the replay buffer  $\mathcal{D}$ . Both the critic

and actor networks are updated through gradient descent, according to the loss functions defined in Eqs. (9) and (25), respectively. Additionally, the parameters of the target critic networks are updated in a smooth mechanism using a soft update mechanism controlled by the parameter  $\rho$ .

After these updates, the algorithm proceeds to the next timestep. This iterative process continues until the training is completed, leading to the learned critic networks  $Q^{\theta_1}(\cdot)$ ,  $Q^{\theta_2}(\cdot)$ , and actor network  $\pi^{\phi}(\cdot)$ .

## IV. EXPERIMENTS

### A. Experimental Settings

As illustrated in Fig.1 and Table II, the performance of the proposed CSAC algorithm was rigorously evaluated across four benchmark control tasks within the MuJoCo physics engine [39], [40], namely HalfCheetah-v4 (17-dimensional state, 6-dimensional action), Walker2d-v4 (17-dimensional state, 6-dimensional action), Ant-v4 (27-dimensional state, 8-dimensional action), and Hopper-v4 (11-dimensional state, 3-dimensional action). These tasks were meticulously chosen to encompass a diverse set of robotic structures and dynamic control challenges, thereby providing a comprehensive assessment of CSAC’s robustness and generalizability.

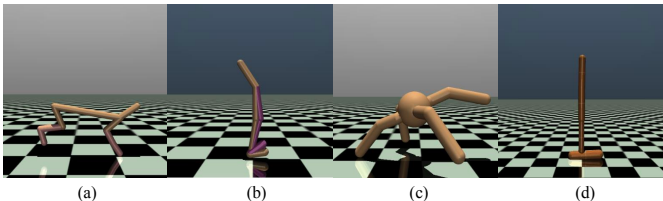


Fig. 1. Benchmark tasks for evaluation in this article. (a) HalfCheetah-v4. (b) Walker2d-v4. (c) Ant-v4. (d) Hopper-v4.

TABLE II  
OBSERVATION AND ACTION SPACES FOR DIFFERENT MUJOCo TASKS

	Observation Space	Action Space
HalfCheetah-v4	17	6
Walker2d-v4	17	6
Ant-v4	27	8
Hopper-v4	11	3

To establish a comparative baseline, we selected four prominent Actor-Critic (AC) reinforcement learning algorithms: Soft Actor-Critic (SAC) [19], Proximal Policy Optimization (PPO) [25], Twin Delayed Deep Deterministic Policy Gradient (TD3) [30], and the recent state-of-the-art Softmax Deep Double Deterministic Policy Gradient (SD3) [41]. These algorithms represent a range of on-policy and off-policy approaches, enabling a robust comparison. All experimental outcomes were derived from five independent trials per task, ensuring statistical rigor and minimizing the influence of stochastic variability.

The CSAC implementation was realized using the PaddlePaddle [42] deep learning framework, leveraging its reinforcement learning toolkit, PARL<sup>1</sup>. The computational experiments were performed on a high-performance server, equipped with an Intel Xeon Gold-6248R CPU, an NVIDIA GeForce RTX-A5000 GPU, and 256 GB of RAM, running Ubuntu 20.04 OS. Such a configuration ensured that the experiments could be executed efficiently and without computational bottlenecks.

The hyperparameters common to all compared algorithms are comprehensively outlined in Table III. These include key settings such as learning rates and the network architectures for both actor and critic networks. For the CSAC algorithm, additional specific parameters were introduced: the entropy regularization coefficient,  $\sigma$ , was uniformly set to 0.2 across all tasks, while the relative entropy regularization parameter,  $\tau$ , was assigned a value of 0.5 for all MuJoCo-based experiments. These parameters were carefully selected to optimize the balance between exploration and exploitation, ensuring that CSAC could effectively navigate the trade-offs inherent in reinforcement learning.

### B. Evaluation of Learning Capability on MuJoCo Tasks

The learning capability of the proposed method was illustrated by the learning curves in Fig. 2 and the average returns in Table IV (the number in red indicated the best performance among all approaches). It clearly demonstrates the significant advantages of the CSAC algorithm across multiple environments.

In the HalfCheetah-v4 task, CSAC consistently outperformed all other algorithms across all timesteps, achieving a final average return of 11672.74, which represents an approximately 5.6% improvement over SAC’s 11052.89 and a nearly 2.79-fold increase compared to PPO’s 4181.89. Compared to TD3 and SD3, CSAC’s performance improved by approximately 41.9% and 63.0%, respectively. These results indicate that CSAC effectively explores and converges stably when handling high-dimensional control problems with complex dynamics.

In the Walker2d-v4 task, CSAC also exhibited superior performance, with an average return of 4106.21, which is approximately 51.5% higher than SAC’s 2710.65. Compared to PPO’s 2403.55, CSAC’s performance improved by about 70.9%. When compared to TD3 and SD3, CSAC demonstrated increases of approximately 16.9% and 20.6%, respectively. This could be attributed to the high difficulty of balancing and gait control in Walker2d-v4, where CSAC’s relative entropy regularization effectively mitigated excessive policy updates, enhancing the algorithm’s robustness.

The results from the Ant-v4 task further validate the effectiveness of CSAC. In this task, CSAC achieved an average return of 5538.20, which is approximately 5.9% higher than SAC’s 5229.39, and significantly outperformed PPO (1836.47) by about 3.02 times. Compared to TD3 (2368.35) and SD3 (2960.61), CSAC improved by approximately 133.9% and 87.1%, respectively. This suggests that CSAC better balances

<sup>1</sup><https://github.com/PaddlePaddle/PARL>

TABLE III  
COMMON HYPER-PARAMETER SETTINGS OF COMPARED APPROACHES

	CSAC(ours)	SAC	PPO	TD3	SD3
Critic Learning Rate	$3 \cdot 10^{-4}$	$3 \cdot 10^{-4}$	$3 \cdot 10^{-4}$	$3 \cdot 10^{-4}$	$1 \cdot 10^{-3}$
Actor Learning Rate	$3 \cdot 10^{-4}$	$3 \cdot 10^{-4}$	$3 \cdot 10^{-4}$	$3 \cdot 10^{-4}$	$1 \cdot 10^{-3}$
Actor and Critic Structure	(256,256)	(256,256)	(64,64)	(256,256)	(256,256)
Target Update Rate	0.005	0.005	/	0.005	0.005
Batch Size	256	256	32	256	256
Memory Size	$1 \cdot 10^6$	$1 \cdot 10^6$	/	$1 \cdot 10^6$	$1 \cdot 10^6$
Warmup Steps	$1 \cdot 10^4$	$1 \cdot 10^4$	/	$1 \cdot 10^4$	$1 \cdot 10^4$
Discount Factor	0.99	0.99	0.99	0.99	0.99

exploration and exploitation in complex multi-legged robotic tasks, ensuring continuous policy optimization.

In the Hopper-v4 task, although CSAC’s performance was close to that of SD3 (3458.22 vs. 3515.30), it still demonstrated relative superiority, improving by approximately 13.9% over SAC’s 3037.19 and by about 56.9% over PPO’s 2204.01. Compared to TD3 (3296.80), CSAC achieved an increase of approximately 4.9%. While SD3 also performed well in this task, CSAC showed greater stability and robustness across multiple metrics.

In summary, CSAC exhibited outstanding performance across several classic MuJoCo tasks, largely due to the introduction of relative entropy regularization in the algorithm. This regularization contributed to a more balanced policy update process, effectively enhancing both exploration capabilities and convergence speed. The experimental results demonstrate that CSAC possesses broad applicability and superior performance in complex continuous control tasks.

### C. Ablation Study on Walker2d Task

In this study, we conducted a detailed evaluation of the impact of different relative entropy hyperparameters ( $\tau$ ) on the performance of the CSAC algorithm in the Walker2d-v4 environment. Given that the influence of entropy hyperparameters on algorithm performance has been extensively discussed in SAC-related literature [19], [43], our analysis specifically focuses on the role of relative entropy hyperparameters in CSAC.

The experimental results, illustrated in the accompanying Fig.3, present the variation in average returns within one million timesteps under different  $\tau$  settings, ranging from 0.005 to 50.0.

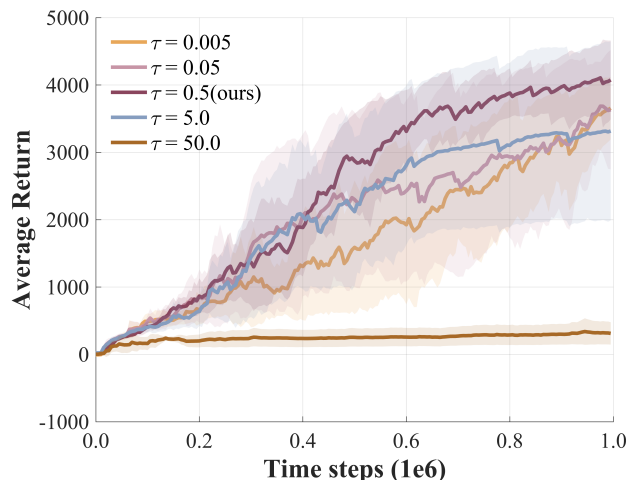


Fig. 3. Learning curves of CSAC with different  $\tau$  values in the Walker2d-v4 task. The shaded region represents the standard deviation of the average evaluation over five trials. Curves are smoothed uniformly for visual clarity.

Our observations indicate that the value of  $\tau$  has a significant impact on the algorithm’s performance. Notably, a larger  $\tau$  value implies a stronger constraint on the algorithm due to relative entropy, meaning that larger  $\tau$  values impose stricter limits on the deviation from the previous policy during updates, thereby making the policy more conservative.

When  $\tau$  is set to smaller values (e.g.,  $\tau = 0.005$  and  $\tau = 0.05$ ), the algorithm exhibits slower growth in average returns, and the final return values are relatively low. This could be attributed to the insufficient constraint imposed by small  $\tau$  values during policy updates. In our algorithm, relative entropy is implemented as reverse KL divergence, and smaller  $\tau$  values weaken the impact of reverse KL divergence on the algorithm. Reverse KL divergence tends to focus on high-probability regions of the new policy, which may reduce the algorithm’s exploratory capabilities. Consequently, the policy exhibits weaker exploration and ultimately suboptimal convergence.

Conversely, when  $\tau$  is set to a moderate range, such as  $\tau = 0.5$  (the default setting in our algorithm), the algorithm performs optimally. The results demonstrate that with  $\tau = 0.5$ , the CSAC algorithm consistently achieves the highest average returns throughout the training process, with final

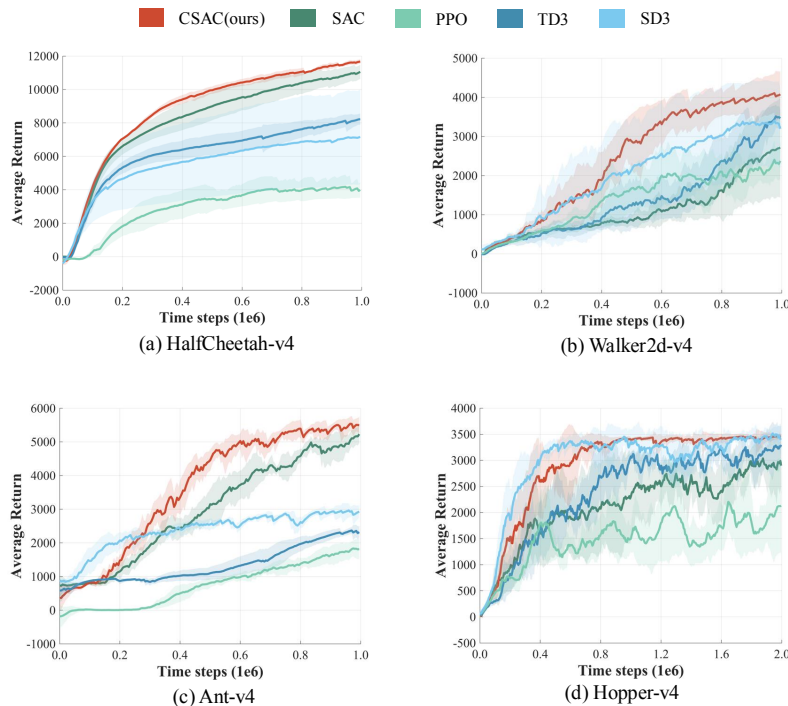


Fig. 2. Learning curves over four benchmark tasks. Curves are uniformly smoothed for visual clarity. The shaded region represents the corresponding standard deviation.

TABLE IV  
MAXIMUM AVERAGE RETURNS OVER FOUR BENCHMARK TASKS

	<b>CSAC (ours)</b>	<b>SAC</b>	<b>PPO</b>	<b>TD3</b>	<b>SD3</b>
HalfCheetah-v4	<b>11672.74 ± 151.21</b>	11052.89 ± 422.84	4181.89 ± 723.54	8224.70 ± 337.13	7158.19 ± 2821.74
Walker2d-v4	<b>4106.21 ± 501.45</b>	2710.65 ± 1272.01	2403.55 ± 502.86	3513.25 ± 295.81	3404.03 ± 989.50
Ant-v4	<b>5538.20 ± 209.62</b>	5229.39 ± 269.52	1836.47 ± 233.91	2368.35 ± 99.15	2960.61 ± 212.54
Hopper-v4	3458.22 ± 59.87	3037.19 ± 242.06	2204.01 ± 540.71	3296.80 ± 356.86	<b>3515.30 ± 107.84</b>

returns approaching 4000, significantly outperforming other  $\tau$  settings. This outcome suggests that, in the Walker2d-v4 task, a moderate  $\tau$  value effectively balances exploration and exploitation, enabling the algorithm to explore new policy spaces efficiently while avoiding the instability associated with excessive exploration.

However, as  $\tau$  is further increased, for instance, to  $\tau = 5.0$  and  $\tau = 50.0$ , a decline in algorithm performance is observed. Particularly at  $\tau = 50.0$ , the algorithm's returns almost stagnate at a low level, failing to learn effective policies. This is likely due to the excessively strong constraint imposed by a large  $\tau$  value, which severely limits policy updates, rendering the policy overly conservative and unable to fully exploit the policy space, ultimately leading to a decrease in performance.

In summary, selecting an appropriate relative entropy hyperparameter  $\tau$  is crucial for the success of the CSAC algorithm in the Walker2d-v4 task. The experimental results indicate that  $\tau = 0.5$  provides the optimal performance, allowing the algorithm to maintain a balance between exploration and stable, efficient convergence. In contrast, both excessively small and large  $\tau$  values lead to performance degradation, underscoring the need to adjust  $\tau$  appropriately based on

the specific task context to achieve optimal policy learning outcomes.

#### D. Evaluation of Sample Efficiency

In this subsection, we define the sample efficiency as the number of interactions used by each approach to reach the lower boundary of the maximum average returns in Table IV. It is crucial to the implementation of RL to real-world hardware with extremely high sampling costs. The sampling efficiency of the proposed method was evaluated in Fig. 4 and Table V (the number in red indicated the best performance among all approaches).

The experimental results demonstrate that the CSAC algorithm exhibits exceptional sample efficiency across all four tasks. In the HalfCheetah-v4 task, CSAC required only 105,000 steps to achieve the target return, which is an 8.7% reduction compared to the 115,000 steps needed by SAC, a 22.2% reduction compared to the 135,000 steps required by TD3, and an 8.05-fold improvement over the 950,000 steps needed by PPO. When compared to SD3, which required 165,000 steps, CSAC reduced the step requirement by 36.4%.

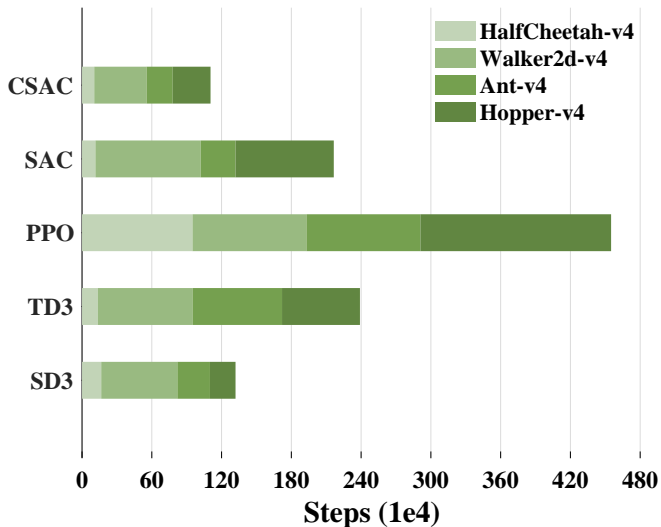


Fig. 4. Number of interactions used by all compared approaches to reach the lower boundary of the maximum average returns over four benchmark control tasks.

TABLE V  
NUMBER OF INTERACTIONS REQUIRED TO REACH THE LOWER BOUND OF MAXIMUM AVERAGE RETURN (IN  $10^4$  STEPS)

	HalfCheetah-v4	Walker2d-v4	Ant-v4	Hopper-v4
CSAC	<b>10.5</b>	<b>45</b>	<b>22.5</b>	32.5
SAC	11.5	90.5	30	84.5
PPO	95	98	98	164
TD3	13.5	81.5	77	67
SD3	16.5	65.5	28	<b>22</b>

Similarly, in the Walker2d-v4 task, CSAC demonstrated significant advantages, requiring only 450,000 steps to reach the target return. In contrast, SAC required 905,000 steps, giving CSAC a 50.3% efficiency improvement. Compared to TD3, which required 815,000 steps, CSAC reduced the step requirement by 44.8%, and compared to PPO, which needed 980,000 steps, CSAC’s efficiency improved by 1.18 times. Although SD3 performed relatively well at 655,000 steps, CSAC still maintained a 31.3% efficiency advantage.

For the Ant-v4 task, CSAC reached the target return in 225,000 steps, significantly outperforming SAC’s 300,000 steps with a 25% improvement in sample efficiency. Compared to TD3’s 770,000 steps, CSAC reduced the step requirement by 70.8%, and compared to PPO’s 980,000 steps, CSAC’s efficiency increased by 3.36 times. Even though SD3 required 280,000 steps for this task, CSAC still demonstrated a 19.6% efficiency advantage.

In the Hopper-v4 task, CSAC required 325,000 steps to reach the lower bound of the maximum average return, which represents a 61.5% reduction in steps compared to SAC’s 845,000 steps and a 4.05-fold improvement over PPO’s 1,640,000 steps. Although SD3 performed the best in this task, requiring only 220,000 steps, CSAC still maintained a high level of competitiveness, falling only slightly behind SD3.

In summary, the joint regularization of entropy and relative entropy significantly contributes to the superior sample

efficiency of the CSAC algorithm across multiple MuJoCo tasks, particularly in the HalfCheetah-v4 and Walker2d-v4 tasks. Compared to other mainstream reinforcement learning algorithms, CSAC consistently achieves target returns with fewer environment interaction steps, indicating its ability to effectively balance exploration and exploitation, rapidly converge to optimal policies, and substantially reduce the sample requirements for training. The experimental results further suggest that CSAC not only possesses significant performance advantages in complex, high-dimensional tasks but also demonstrates broad applicability and stability in terms of sample efficiency.

#### E. Evaluation of Robustness in HalfCheetah Task

In this study, we conducted an in-depth analysis of the stability of the CSAC algorithm, particularly within the HalfCheetah-v4 environment. We introduced varying levels of dynamic noise to assess the algorithm’s adaptability and robustness in dynamically changing conditions. Specifically, after 300,000 steps of standard training, the environmental friction was suddenly increased to 1.5, 2.0, and 2.5 times its original value to simulate the impact of different intensities of dynamic noise. Typically, an increase in friction corresponds to a higher task difficulty, with stronger noise being induced by larger changes in friction. Therefore, the performance of the algorithm under these conditions effectively reflects its stability and ability to cope with complex environments.

In this experiment, we chose to compare CSAC with the SAC algorithm, primarily due to their structural similarities; both algorithms leverage entropy regularization to promote policy exploration. However, CSAC enhances the stability and efficacy of policy updates by incorporating relative entropy regularization, which is expected to confer greater robustness and adaptability in environments with dynamic noise. By directly comparing CSAC with SAC, we can more clearly analyze the contribution of relative entropy regularization to algorithm stability, while avoiding potential performance biases that might arise from differences in algorithmic architecture.

The experimental results, as depicted in the accompanying Fig. 5, reveal several key findings. When friction was increased to 1.5 times its original value (left panel, Evaluation Stage 1), both CSAC and SAC exhibited fluctuations in returns during training. However, CSAC was able to quickly adjust its policy, leading to a recovery in returns that eventually surpassed those of SAC. During the evaluation phase, CSAC maintained stable performance, slightly outperforming SAC. This indicates that CSAC possesses a strong capacity for adaptation under moderate levels of dynamic noise, effectively adjusting its policy while maintaining a high level of performance.

As the friction multiplier increased to 2.0 (middle panel, Evaluation Stage 2), corresponding to a significant rise in task difficulty and noise intensity, SAC’s performance became increasingly erratic, with a slower recovery in returns. In contrast, although CSAC was also affected by the environmental change, it exhibited a much faster recovery. Throughout subsequent training and evaluation phases, CSAC consistently maintained a higher level of returns, whereas SAC continued

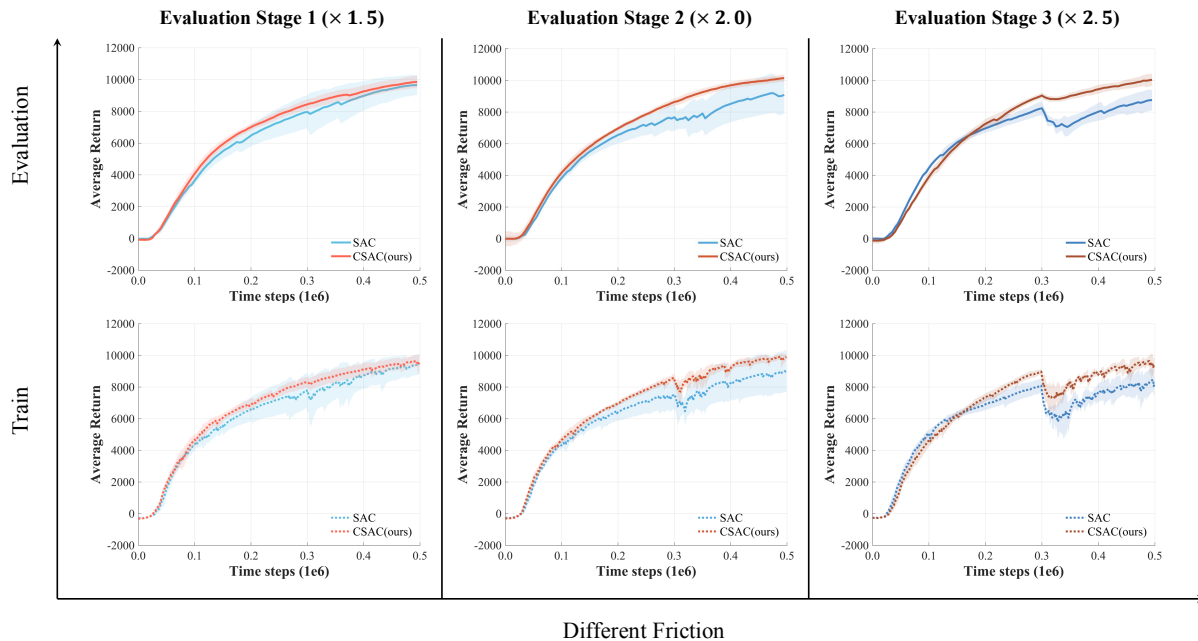


Fig. 5. Performance comparison of CSAC and SAC under varying Friction-Induced dynamic noise in the HalfCheetah-v4 environment. The shaded region represents the corresponding standard deviation.

to fluctuate, failing to reach comparable performance levels. Notably, during the evaluation phase, CSAC demonstrated a significant advantage over SAC, highlighting its superior robustness and adaptability. These results suggest that CSAC retains its strategic advantage and stability even when confronted with higher levels of difficulty and noise.

When the friction multiplier was further increased to 2.5 (right panel, Evaluation Stage 3), the experimental conditions reached maximum difficulty. Both CSAC and SAC experienced a noticeable decline in returns during training; however, CSAC’s performance was notably better, with a smaller decline and a quicker adaptation to the new environmental conditions. In contrast, SAC exhibited more severe fluctuations in returns, with a slower recovery compared to CSAC. During the evaluation phase, CSAC once again demonstrated its exceptional stability, with returns gradually stabilizing at a higher level, while SAC showed significant instability and struggled to recover to its initial performance levels. This further validates the robustness and superior performance of CSAC in the face of extreme dynamic noise.

In summary, the experimental results indicate that the CSAC algorithm demonstrates exceptional stability and robustness in the HalfCheetah-v4 environment, regardless of whether it is faced with moderate (1.5x friction) or high-intensity (2.5x friction) dynamic noise. CSAC not only rapidly adapts to environmental changes, maintaining high-level policy performance in challenging tasks, but also consistently outperforms SAC in terms of recovery speed and stability during both training and evaluation phases. The direct comparison with SAC further corroborates the effectiveness of relative entropy regularization in enhancing policy stability and robustness in dynamically changing environments.

## F. Implementation on Real-Robot-Based Simulation

1) *Experimental Settings for Real-Robot-Based Simulation Experiments:* In this experiment, we employed two PyBullet-based simulation platforms [44], PyFlyt [45] and Panda Gym [46], to evaluate the performance of the CSAC algorithm in Real-Robot-Based simulations. The specific experimental setups are illustrated in Fig. 6 and detailed in Table VI.

The first experiment was conducted using the PyFlyt simulation platform, focusing on the QuadX-Waypoints-v1 task (Fig. 6a). This task involves controlling a quadrotor UAV (QuadX) to navigate through a series of waypoints. The goal of the environment is to efficiently control the four rotors of the UAV to guide it through four designated waypoints as quickly as possible. The observation space for this environment consists of 24 dimensions, while the action space comprises 4 dimensions. Fig. 6a (left) provides a schematic representation of the task environment, and Fig. 6a (right) shows a sample trajectory of a trained UAV successfully navigating through the waypoints.

The second experiment was performed on the Panda Gym simulation platform, centered on the PandaReach-v2 task (Fig. 6b). This task requires controlling multiple joints of a Panda robotic arm to move its end-effector to a target position as quickly as possible. Panda Gym is specifically designed for testing reinforcement learning algorithms in robotic manipulation tasks, offering various environments such as grasping, stacking, and path planning. The observation space in PandaReach-v2 consists of 9 dimensions, with an action space of 4 dimensions.

The common parameters for both robotics experiments were configured according to Table III. For the CSAC algorithm, specific parameters, including the  $\sigma$  value controlling entropy and the  $\tau$  value regulating relative entropy regularization, are

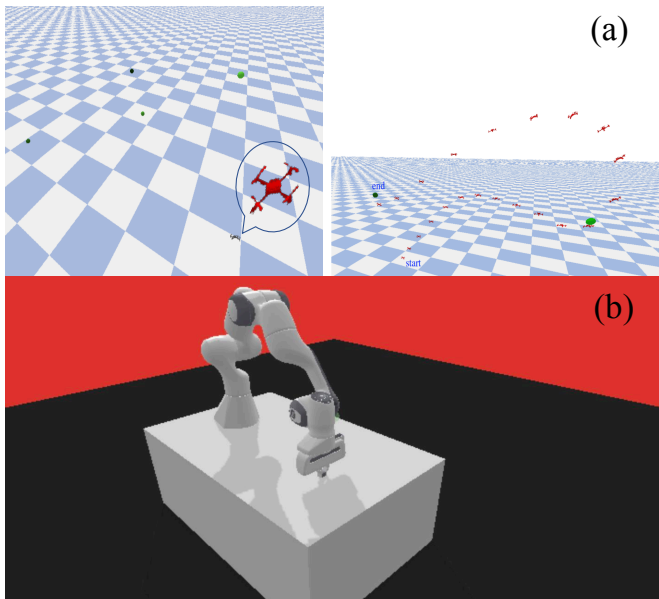


Fig. 6. Real-Robot-Based simulation experiments for evaluation in this article. (a) QuadX-Waypoints-v1. (b) PandaReach-v2.

TABLE VI  
OBSERVATION AND ACTION SPACES FOR TWO REAL-ROBOT-BASED SIMULATION TASKS

	Observation Space	Action Space
QuadX-Waypoints-v1	9	4
PandaReach-v2	17	6

detailed in Table VII. Additionally, to ensure the reliability of the results, all experiments were conducted over five independent trials, with the reported outcomes being the averaged results.

TABLE VII  
SPECIFIC HYPERPARAMETERS OF CSAC

	$\sigma$	$\tau$
QuadX-Waypoints-v1	0.2	0.1
PandaReach-v2	0.2	0.5

2) *Evaluation of the Learning Capability on Two Real-Robot-Based Simulation Tasks:* In this experiment, we evaluated the learning performance of the CSAC algorithm and conducted a comprehensive comparison with the state-of-the-art algorithms, including SAC, PPO, TD3, and SD3. The results are summarized in Fig. 7 and Table VIII (the number in red indicated the best performance among all approaches).

In the QuadX-Waypoints-v1 task, the CSAC algorithm demonstrated superior performance throughout the training process, achieving a final average return of 530.28, which is significantly higher than those of the other compared algorithms. Specifically, CSAC's average return was approximately 36.5% higher than that of SAC and 22.3% higher than TD3. Notably, CSAC exhibited an improvement of approximately 98.6% over PPO, nearly doubling its performance. Addi-

tionally, CSAC outperformed SD3 by 38.5%. These results indicate that CSAC offers significant advantages in terms of sample efficiency and return stability, particularly in more complex environments where it exhibits greater robustness.

In the PandaReach-v2 task, CSAC again exhibited outstanding performance. Although this task is relatively simple, it demands a higher degree of precision in control. The experimental results revealed that CSAC achieved a final average return of -2.04, slightly improving upon SAC's -2.12. It is worth noting that PPO, TD3, and SD3 performed poorly in this task, with average returns of -49.80, -48.57, and -48.36, respectively, highlighting their significant deficiencies in handling tasks that require high precision. While CSAC's performance in this task was close to that of SAC, it demonstrated better return stability with lower variance, further validating its robustness in fine control tasks.

In summary, the CSAC algorithm consistently outperformed the other compared algorithms across both tasks, showing marked advantages in sample efficiency and return stability. In the QuadX-Waypoints-v1 task, CSAC improved by 36.5% over SAC and nearly doubled the performance of PPO. In the PandaReach-v2 task, CSAC's performance was nearly 24 times better than that of PPO, further corroborating its robustness and effectiveness in complex control tasks. Overall, these results suggest that the CSAC algorithm exhibits broad adaptability and superior performance, making it highly applicable to a wide range of reinforcement learning scenarios.

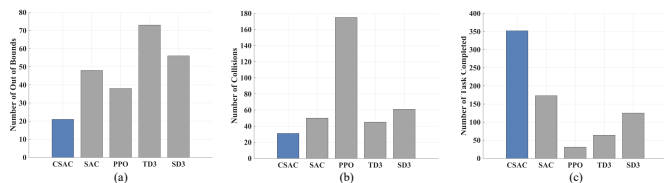


Fig. 8. The average number of each condition in QuadX-Waypoints-v1: (a) Number of out of bounds; (b) Number of collisions; (c) Number of task completed.

TABLE IX  
CASE ANALYSIS IN QUADX-WAYPOINTS-V1

	Out of Bound	Collision	Completion
CSAC	<b>20.6 ± 11.24</b>	<b>31.6 ± 10.41</b>	<b>352.0 ± 241.57</b>
SAC	48.2 ± 27.54	50.6 ± 14.36	173.4 ± 230.56
PPO	38.4 ± 17.93	175.4 ± 4.16	31.0 ± 19.67
TD3	73.2 ± 20.5	45.4 ± 15.01	64.0 ± 68.31
SD3	56.0 ± 18.72	61.2 ± 24.34	125.4 ± 158.86

3) *Evaluation of Robustness in Drones Control:* We further investigated the impact of CSAC on the robustness of learned control policy in the QuadX-Waypoints-v1. In this task, five evaluation rollouts were conducted every 5,000 steps with the current policy. We summarized the condition of these rollouts (1000 rollouts in one learning) including out-of-bounds, collision, and successful completion among all compared approaches and all trials. The experiments were based on a

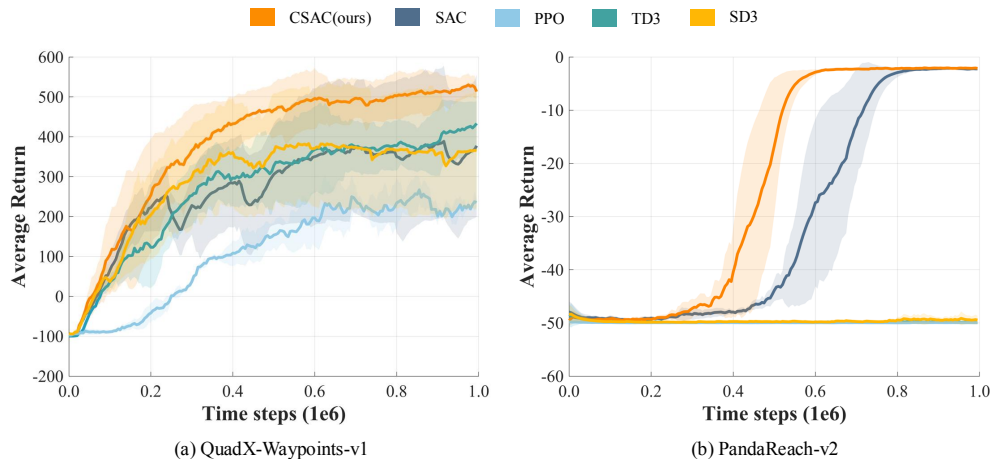


Fig. 7. Learning curves of two Real-Robot-Based simulation tasks. The shaded region represents the standard deviation of the average evaluation over five independent trials. Curves are uniformly smoothed for visual clarity.

TABLE VIII  
MAX AVERAGE RETURNS OVER TWO REAL-ROBOT-BASED SIMULATION TASKS

	CSAC (ours)	SAC	PPO	TD3	SD3
QuadX-Waypoints-v1	<b>530.28 ± 29.04</b>	388.55 ± 189.51	267.06 ± 32.07	433.56 ± 56.03	383.03 ± 145.51
PandaReach-v2	<b>-2.04 ± 0.18</b>	-2.12 ± 0.22	-49.80 ± 0.04	-48.57 ± 0.08	-48.36 ± 0.10

total of five randomized experiments. The average number of each condition was demonstrated in Fig. 9 and Table IX (the number in red indicated the superior performances).

It is observed that the proposed CSAC enjoyed great robustness in controlling drones. With the regularization terms of both entropy and relative entropy, CSAC could have an effective exploration policy while avoiding over-large policy updates which may result in unstable situations. It achieved the lowest number of failed rollouts caused by driving out of bound and collision and had the most successful completion of the evaluation rollouts than other baselines. In avoiding unstable situations, CSAC reduced 46.3% out of bound than the suboptimal method PPO and reduced 30.4% collision than the suboptimal method TD3. It controlled drones to successfully pass the evolution rollout over 350 times, close to the sum of the number of successful rollouts using four baselines. This result demonstrated the advantage of our proposed method in reducing control task failure cases while considering safety and stability.

4) *Evaluation of Effectiveness in Robotic Arm:* In this section, we conducted a further evaluation of the CSAC algorithm's performance on the PandaReach-v2 task. The primary metric for this experiment was the average success rate, which reflects the learning efficiency and final performance of the algorithm as training progresses.

As illustrated in the figure, the CSAC algorithm demonstrated a clear advantage throughout the training process. Initially, all algorithms exhibited low success rates, indicating the high difficulty of the task and the ineffectiveness of early-stage policy learning. However, as training progressed, CSAC's success rate began to rise rapidly around 400,000 steps and reached nearly 100% by approximately 600,000

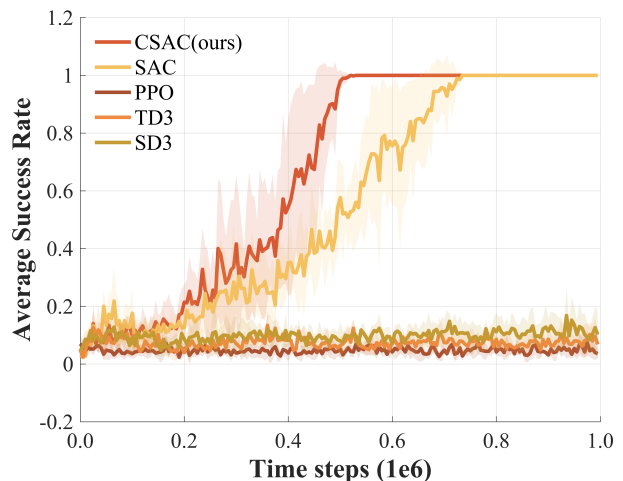


Fig. 9. The average success rate in PandaReach-v2.

steps. This result indicates that the CSAC algorithm effectively learned the control strategy and achieved optimal performance within a relatively short period.

In contrast, while the SAC algorithm gradually improved its success rate in the later stages of training (around 800,000 steps), its convergence was noticeably slower than that of CSAC, and its final success rate remained slightly lower. The performance of PPO, TD3, and SD3 was significantly inferior to that of both CSAC and SAC, with large fluctuations in success rate throughout training and an inability to achieve effective policy learning. This suggests that these algorithms struggle to meet the high precision control demands of the

PandaReach-v2 task.

In summary, the experimental results demonstrate that the CSAC algorithm possesses significant performance advantages in the PandaReach-v2 task, particularly in terms of the speed of success rate improvement and final convergence performance. CSAC's results confirm its adaptability and effectiveness in high-precision control tasks, far surpassing the other compared algorithms.

## V. CONCLUSIONS

This paper introduces Conservative Soft Actor-Critic (CSAC), an algorithm that integrates both entropy and relative entropy regularization into the Actor-Critic framework. This integration is designed to enhance the effectiveness and stability of reinforcement learning in robot control tasks. We evaluated CSAC on four benchmark control tasks and two real-robot-based simulation tasks, where it demonstrated superior learning capability, sample efficiency, and robustness compared to state-of-the-art baselines. These results suggest that the joint consideration of entropy and relative entropy is a promising direction for developing more practical reinforcement learning methods.

For future work, we plan to investigate the individual and combined effects of the entropy and relative entropy terms on algorithm performance. Specifically, we aim to explore how these regularization terms influence the stability and convergence of the learning process. Additionally, we intend to develop an adaptive strategy for parameter selection, where the parameters  $\rho$  and  $\tau$  will be adjusted dynamically to optimize the trade-off between exploration and exploitation.

In terms of engineering application, our next step is to implement CSAC on real-world hardware, including unmanned aerial vehicles (UAVs) and other robotic systems. This will allow us to evaluate the algorithm's effectiveness under real-world conditions, where challenges such as real-time decision-making and physical constraints are more pronounced. These implementations will help bridge the gap between simulation-based research and practical applications in robotics.

## REFERENCES

- [1] R. S. Sutton and A. G. Barto, *Reinforcement learning: An introduction*. MIT press, 2018.
- [2] J. Kober, J. A. Bagnell, and J. Peters, "Reinforcement learning in robotics: A survey," *The International Journal of Robotics Research*, vol. 32, no. 11, pp. 1238–1274, 2013.
- [3] V. Mnih, K. Kavukcuoglu, D. Silver, A. A. Rusu, J. Veness, M. G. Bellemare, A. Graves, M. Riedmiller, A. K. Fidjeland, G. Ostrovski, et al., "Human-level control through deep reinforcement learning," *Nature*, vol. 518, no. 7540, pp. 529–533, 2015.
- [4] D. Silver, T. Hubert, J. Schrittwieser, I. Antonoglou, M. Lai, A. Guez, M. Lanctot, L. Sifre, D. Kumaran, T. Graepel, et al., "A general reinforcement learning algorithm that masters chess, shogi, and go through self-play," *Science*, vol. 362, no. 6419, pp. 1140–1144, 2018.
- [5] E. Kaufmann, L. Bauersfeld, A. Loquercio, M. Müller, V. Koltun, and D. Scaramuzza, "Champion-level drone racing using deep reinforcement learning," *Nature*, vol. 620, no. 7976, pp. 982–987, 2023.
- [6] Z. Wang, Y. Jia, L. Shi, H. Wang, H. Zhao, X. Li, J. Zhou, J. Ma, and G. Zhou, "Arm-constrained curriculum learning for loco-manipulation of the wheel-legged robot," *arXiv preprint arXiv:2403.16535*, 2024.
- [7] C. Miao, Y. Cui, H. Li, and X. Wu, "Effective multi-agent deep reinforcement learning control with relative entropy regularization," *IEEE Transactions on Automation Science and Engineering*, 2024.
- [8] I. Goodfellow, Y. Bengio, and A. Courville, *Deep learning*. MIT Press, 2016.
- [9] T. P. Lillicrap, J. J. Hunt, A. Pritzel, N. Heess, T. Erez, Y. Tassa, D. Silver, and D. Wierstra, "Continuous control with deep reinforcement learning," in *International Conference on Learning Representations (ICLR)*, 2016.
- [10] L. Zhu, Y. Cui, and T. Matsubara, "Dynamic actor-advisor programming for scalable safe reinforcement learning," in *2020 IEEE International Conference on Robotics and Automation (ICRA)*, pp. 10681–10687, IEEE, 2020.
- [11] Y. Cui, S. Osaki, and T. Matsubara, "Autonomous boat driving system using sample-efficient model predictive control-based reinforcement learning approach," *Journal of Field Robotics*, vol. 38, no. 3, pp. 331–354, 2021.
- [12] D. Chen, H. Li, Z. Jin, and H. Tu, "Risk-anticipatory autonomous driving strategies considering vehicles' weights, based on hierarchical deep reinforcement learning," *arXiv preprint arXiv:2401.08661*, 2023.
- [13] R. Yan, R. Jiang, B. Jia, J. Huang, and D. Yang, "Hybrid car-following strategy based on deep deterministic policy gradient and cooperative adaptive cruise control," *IEEE Transactions on Automation Science and Engineering*, vol. 19, no. 4, pp. 2816–2824, 2021.
- [14] B. Cai, C. Wei, and Z. Ji, "Deep reinforcement learning with multiple unrelated rewards for agv mapless navigation," *IEEE Transactions on Automation Science and Engineering*, 2024.
- [15] Y. Zhou, Y. Jin, P. Lu, S. Jiang, Z. Wang, and B. He, "T-td3: A reinforcement learning framework for stable grasping of deformable objects using tactile prior," *IEEE Transactions on Automation Science and Engineering*, 2024.
- [16] H. Zhu, J. Yu, A. Gupta, D. Shah, K. Hartikainen, A. Singh, V. Kumar, and S. Levine, "The ingredients of real world robotic reinforcement learning," in *International Conference on Learning Representations*, 2020.
- [17] G. Dulac-Arnold, N. Levine, D. J. Mankowitz, J. Li, C. Paduraru, S. Gowal, and T. Hester, "Challenges of real-world reinforcement learning: definitions, benchmarks and analysis," *Machine Learning*, vol. 110, no. 9, pp. 2419–2468, 2021.
- [18] O. Kroemer, S. Niekum, and G. Konidaris, "A review of robot learning for manipulation: Challenges, representations, and algorithms," *Journal of machine learning research*, vol. 22, no. 30, pp. 1–82, 2021.
- [19] T. Haarnoja, A. Zhou, P. Abbeel, and S. Levine, "Soft actor-critic: Off-policy maximum entropy deep reinforcement learning with a stochastic actor," in *International conference on machine learning*, pp. 1861–1870, PMLR, 2018.
- [20] R. Ma, Y. Wang, S. Wang, L. Cheng, R. Wang, and M. Tan, "Sample-observed soft actor-critic learning for path following of a biomimetic underwater vehicle," *IEEE Transactions on Automation Science and Engineering*, pp. 1–10, 2023.
- [21] A. Wahid, A. Stone, K. Chen, B. Ichter, and A. Toshev, "Learning object-conditioned exploration using distributed soft actor critic," in *Conference on Robot Learning*, pp. 1684–1695, PMLR, 2021.
- [22] Z. He, L. Dong, C. Song, and C. Sun, "Multiagent soft actor-critic based hybrid motion planner for mobile robots," *IEEE transactions on neural networks and learning systems*, 2022.
- [23] K. Nakhleh, M. Raza, M. Tang, M. Andrews, R. Boney, I. Hadžić, J. Lee, A. Mohajeri, and K. Palyutina, "Sacplanner: Real-world collision avoidance with a soft actor critic local planner and polar state representations," in *2023 IEEE International Conference on Robotics and Automation (ICRA)*, pp. 9464–9470, IEEE, 2023.
- [24] J. Schulman, S. Levine, P. Abbeel, M. Jordan, and P. Moritz, "Trust region policy optimization," in *International conference on machine learning*, pp. 1889–1897, PMLR, 2015.
- [25] J. Schulman, F. Wolski, P. Dhariwal, A. Radford, and O. Klimov, "Proximal policy optimization algorithms," *arXiv preprint arXiv:1707.06347*, 2017.
- [26] D. Xue, D. Wu, A. S. Yamashita, and Z. Li, "Proximal policy optimization with reciprocal velocity obstacle based collision avoidance path planning for multi-unmanned surface vehicles," *Ocean Engineering*, vol. 273, p. 114005, 2023.
- [27] P. Sadhukhan and R. R. Selmic, "Multi-agent formation control with obstacle avoidance using proximal policy optimization," in *2021 IEEE International Conference on Systems, Man, and Cybernetics (SMC)*, pp. 2694–2699, IEEE, 2021.
- [28] Y. Guan, Y. Ren, S. E. Li, Q. Sun, L. Luo, and K. Li, "Centralized cooperation for connected and automated vehicles at intersections by proximal policy optimization," *IEEE Transactions on Vehicular Technology*, vol. 69, no. 11, pp. 12597–12608, 2020.

- [29] E. Bøhn, E. M. Coates, S. Moe, and T. A. Johansen, "Deep reinforcement learning attitude control of fixed-wing uavs using proximal policy optimization," in *2019 international conference on unmanned aircraft systems (ICUAS)*, pp. 523–533, IEEE, 2019.
- [30] S. Fujimoto, H. Hoof, and D. Meger, "Addressing function approximation error in actor-critic methods," in *International Conference on Machine Learning (ICML)*, 2018.
- [31] M. G. Azar, V. Gómez, and H. J. Kappen, "Dynamic policy programming," *The Journal of Machine Learning Research*, vol. 13, no. 1, pp. 3207–3245, 2012.
- [32] T. Kozuno, E. Uchibe, and K. Doya, "Theoretical analysis of efficiency and robustness of softmax and gap-increasing operators in reinforcement learning," in *International Conference on Artificial Intelligence and Statistics (AISTATS)*, 2019.
- [33] Y. Cui, T. Matsubara, and K. Sugimoto, "Kernel dynamic policy programming: Applicable reinforcement learning to robot systems with high dimensional states," *Neural Networks*, vol. 94, pp. 13–23, 2017.
- [34] Y. Tsurumine, Y. Cui, E. Uchibe, and T. Matsubara, "Deep reinforcement learning with smooth policy update: Application to robotic cloth manipulation," *Robotics and Autonomous Systems*, vol. 112, pp. 72–83, 2019.
- [35] Z. Shang, H. Li, and Y. Cui, "Shiftable dynamic policy programming for efficient and robust reinforcement learning control," in *2021 IEEE International Conference on Robotics and Biomimetics (ROBIO)*, pp. 1688–1693, IEEE, 2021.
- [36] Z. Shang, R. Li, C. Zheng, H. Li, and Y. Cui, "Relative entropy regularized sample-efficient reinforcement learning with continuous actions," *IEEE Transactions on Neural Networks and Learning Systems*, 2023.
- [37] T. P. Lillicrap, J. J. Hunt, A. Pritzel, N. Heess, T. Erez, Y. Tassa, D. Silver, and D. Wierstra, "Continuous control with deep reinforcement learning," *arXiv preprint arXiv:1509.02971*, 2015.
- [38] T. Haarnoja, H. Tang, P. Abbeel, and S. Levine, "Reinforcement learning with deep energy-based policies," in *International conference on machine learning*, pp. 1352–1361, PMLR, 2017.
- [39] E. Todorov, T. Erez, and Y. Tassa, "Mujoco: A physics engine for model-based control," in *2012 IEEE/RSJ international conference on intelligent robots and systems*, pp. 5026–5033, IEEE, 2012.
- [40] M. Towers, A. Kwiatkowski, J. Terry, J. U. Balis, G. De Cola, T. Deleu, M. Goulão, A. Kallinteris, M. Krimmel, A. KG, *et al.*, "Gymnasium: A standard interface for reinforcement learning environments," *arXiv preprint arXiv:2407.17032*, 2024.
- [41] L. Pan, Q. Cai, and L. Huang, "Softmax deep double deterministic policy gradients," *Advances in Neural Information Processing Systems*, vol. 33, pp. 11767–11777, 2020.
- [42] Y. Ma, D. Yu, T. Wu, and H. Wang, "Paddlepaddle: An open-source deep learning platform from industrial practice," *Frontiers of Data and Computing*, vol. 1, no. 1, pp. 105–115, 2019.
- [43] T. Haarnoja, A. Zhou, K. Hartikainen, G. Tucker, S. Ha, J. Tan, V. Kumar, H. Zhu, A. Gupta, P. Abbeel, *et al.*, "Soft actor-critic algorithms and applications," *arXiv preprint arXiv:1812.05905*, 2018.
- [44] E. Coumans and Y. Bai, "Pybullet, a python module for physics simulation for games, robotics and machine learning." <http://pybullet.org>, 2016–2021.
- [45] J. J. Tai, J. Wong, M. Innocente, N. Horri, J. Brusey, and S. K. Phang, "Pyflyt-uav simulation environments for reinforcement learning research," *arXiv preprint arXiv:2304.01305*, 2023.
- [46] Q. Gallowédec, N. Cazin, E. Dellandréa, and L. Chen, "panda-gym: Open-Source Goal-Conditioned Environments for Robotic Learning," *4th Robot Learning Workshop: Self-Supervised and Lifelong Learning at NeurIPS*, 2021.



**Xinyi Yuan** received the Mphil degree in intelligent transportation from The Hong Kong University of Science and Technology (Guangzhou), Guangzhou, China in 2024. She received the bachelor's degree from the Southern University of Science and Technology, Shenzhen, China in 2022.



**Zhiwei Shang** received the B.S. degree in Hydrology and Water Resources Engineering from the Sichuan University, China, in 2020, and the M.S. degree in Computer Technology from University of Chinese Academy of Sciences, China, in 2023. Currently, he is a research assistant at the Hong Kong University of Science and Technology (Guangzhou), China. His research interests mainly include reinforcement learning and intelligent control.



**Wenjun Huang** received the B.E. degree in industrial engineering from the Harbin University of Commerce, Harbin, China, in 2022. He is currently working toward his M.Sc. degree in computer technology at Shenzhen Institute of Advanced Technology, Chinese Academy of Science, Shenzhen, China. His current research interests include deep reinforcement learning, model-based reinforcement learning and robot control.



**Yunduan Cui** (Member, IEEE) received Ph.D. in computer science from Nara Institute of Science and Technology, Japan in 2017, M.E in computer science from Doshisha University, Japan in 2014, and the B.E. in Electronic Engineering from Xidian University, China in 2012. From 2017 to 2020, he was a post-doctor researcher in Nara Institute of Science and Technology, Japan. He is currently an Associate Professor at Shenzhen Institute of Advanced Technology, Chinese Academy of Sciences, China. His research focuses on the machine learning, especially reinforcement learning-driven unmanned systems.

Dr. Cui received the best oral paper award of IEEE-RAS 16th International Conference on Humanoid Robots in 2016, the best student award of Nara Institute of Science and Technology in 2018, the best paper award of Japanese Neural Network Society (JNNS) in 2018, and the SICE International Young Authors Award for IEEE/RSJ International Conference on Intelligent Robots and Systems (IROS) in 2019.



**Di Chen** received the B.Sc. and M.S. degree in Transportation Engineering from School of Transportation engineering, Tongji University, Shanghai, China. Currently, she is a research assistant in the Department of Electrical and Electronic Engineering of The Hong Kong Polytechnic University. Her research interests include traffic simulation, machine learning methods for autonomous vehicles.



**Meixin Zhu** (Member, IEEE) is a tenure-track Assistant Professor in the Thrust of Intelligent Transportation (INTR) under the Systems Hub at the Hong Kong University of Science and Technology (Guangzhou). He is also an affiliated Assistant Professor in the Civil and Environmental Engineering Department at the Hong Kong University of Science and Technology. He obtained a Ph.D. degree in intelligent transportation at the University of Washington (UW) in 2022. He received his BS and MS degrees in traffic engineering in 2015 and 2018, respectively, from Tongji University. His research interests include Autonomous Driving Decision Making and Planning, Driving Behavior Modeling, Traffic-Flow Modeling and Simulation, Traffic Signal Control, and (Multi-Agent) Reinforcement Learning. He is a recipient of the TRB Best Dissertation Award (AED50) in 2023.